EUROPHYSICS LETTERS 1 April 2006

Europhys. Lett., **74** (1), pp. 188–194 (2006)
DOI: 10.1209/epl/i2005-10493-3

Patterns caused by buckle-driven delamination in desiccated colloidal gels

L. Pauchard

FAST UMR 7608 - bât. 502, Campus Universitaire d'Orsay, 91405 Orsay cedex, France

received 22 July 2005; accepted in final form 2 February 2006
published online 22 February 2006

PACS. 83.80.Hj – Suspensions, dispersions, pastes, slurries, colloids.
PACS. 91.60.Ba – Elasticity, fracture, and flow.
PACS. 68.35.Np – Adhesion.

Abstract. – During desiccation of coatings, stress release results in mechanical instabilities that can occur in successive stages. Indeed cracks can divide a brittle coating into adjacent polygonal cells in response to important stress. We focus here on a later stage during which a delamination process is driven by buckling instability of the adjacent cells due to remanent stress in the layer. In this way we consider a drying colloidal gel in the geometry of a layer coating a substrate. This model system exhibits well-controlled physicochemical properties. We show that, in the final stage of the process, simple observation of partial delaminated cells allows for the determination of the adhesion energy of the system. Particularly, the influence of both the drying rate and the solvent on the process is experimentally studied.

Many phenomena involve delamination: from the biological interest (sheets of cells splitting in embryogenesis [1]), to the geological interest (lithospheric delamination [2]). Delamination of a layer attached to a substrate also exhibits a wide applicability from desiccation of paints to microelectronic materials, through recent studies on crack patterns recognition in paintings [3]. From a fundamental point of view, the buckle-driven delamination is related to both elastic behaviour of shells and fracture mechanics. Complex pattern of blisters were studied in refs. [4–6]. However, only few experimental systems allow for accurate measurements of the different parameters occurring in the delamination process: geometrical and mechanical characteristics of the system, out-of-plane deformations. In this letter we report buckle-driven delamination induced by desiccation of a gelled layer, initially attached to a substrate. In a first stage, homogeneous cracks divide the structure into adjacent cells [7]. Then, since the network is more compressed on the drying face, residual stresses lead to out-of-plane deformations which can lift the edges of the cell and generate concave surface [8]. The model system is well adapted to mechanical measurements and allows us to follow optically the dynamics of the process. We show here that studying partial delaminated patterns at the final stage of the delamination process allows for a quantification of the adhesion energy of the layer on the substrate.

The model system consists in an aqueous suspension of rigid nanolatex particles (diameter $2a = 15\,\text{nm}$) at high particle volume fraction (initially 30%). The suspension is stable in the absence of solvent evaporation. A small amount of the solution is deposited inside a circular

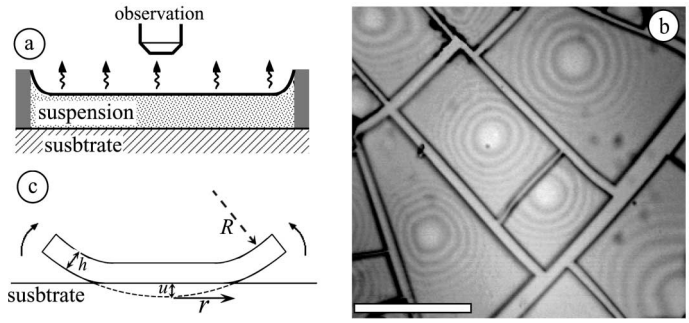

Fig. 1 – a Experimental setup (side view). b Digitized image showing cracks dividing a gelled layer into polygonal cells. Inside a single cell, circular optical interference fringes display an air gap and encircle an adhering region (bright area) (bar = 100 μm). c Idealized sketch (side view) showing a single cell partially delaminated; the radius r of the circular adhering area is related to the so-called indentation, u, of a sphere of radius R by $r \approx \sqrt{2Ru}$ for small u compared to R.

container (diameter = 10 mm) whose bottom is a glass plate and the lateral walls are made of Plexiglas (fig. 1a). The contact line of the solution is quenched at the upper edge of the circular wall and remains there during the whole experiment. In this way we obtain a layer of approximately constant thickness in the center of the container where evaporation is homogeneous, and avoid the anisotropy due to large evaporation at the borders [9]. Under our experimental conditions (absence of convection in the vapour) the transfer of water in air is limited by diffusion and is controlled by the relative humidity, RH, in the surrounding air. During solvent loss, particles accumulate and a gel forms [10]. As the gelled layer dries, it shrinks due to high capillary pressure which can reach a maximum value given by $\frac{2\gamma_{w,a}}{a}$, where $\gamma_{w,a}$ is the water-air surface tension. However, the shrinkage is constrained by the adhesion on the substrate. This growing misfit results in increasing mechanical tensile stress. When the stress exceeds a threshold value, it is released by the formation of cracks which invade the gel. Prior studies [7] have shown that the crack spacing strongly depends on the layer thickness. For layers thick enough, cracks interconnect with each other and divide the structure into polygonal adjacent cells of the surface area denoted by A_{cell}; this quantity will be the parameter of interest in the following, because it can be accurately measured from observations (fig. 1b). Statistics on measurements of A_{cell} have been done as a function of the corresponding cell thickness, h. Reproducible measurements of the layer thickness are performed by detection of a laser beam reflected by the top of the gel surface and a surface of reference. We obtain a scaling law, $A_{cell} \approx \alpha h^2$, in agreement with ref. [7] (α was measured for colloidal gels in different conditions of the desiccation process (table I)). Besides, in order to characterize the elastic properties of the gel, the Young modulus is measured by indentation testing as presented in table I [11](1). The competition between the buckling process and adhesion of the gel on the substrate drives the delamination process.

Since each cell keeps drying from only one surface, a strong stress gradient exists in the layer thickness [10]. As a result, stress reincreases with time and each polygonal cell is compressed in the drying face. When the shrinkage stress reaches a critical value [4] each polygonal cell buckles as its edges lift away from the substrate (fig. 1c). Since the drying gel is transparent,

(1)A spherical tip (diameter = 2 mm) is loaded and results in a penetration depth into a sessile drop of gel (diameter = 20 mm). By recording loading-unloading cycles, the effective Young moduli of our gels were measured just after cracking and before delamination forms. The values obtained are in agreement with previous experiments [12].

TABLE I – *Experimental measurements of the cell surface area, A_{cell} and the Young modulus, Y, in different experimental conditions: desiccation process at $RH = 46\%$ (case 1), $RH = 70\%$ (case 2); in the third case, the suspension is made of an ethanol-water binary mixture $\frac{1}{2} : \frac{1}{2}$ (e, w) and dried at $RH = 46\%$. The main part of the inaccuracy on the adhesion energy by unit area, $\Gamma_{gel/sub}$, comes from the inaccuracy on the Young modulus measurements.*

	1) $RH = 46\%$	2) $RH = 70\%$	3) Solvent e, w
α ($\times 10^{-3}$), $A_{cell} \approx \alpha h^2$	1.8 ± 0.1	2.6 ± 0.2	1.2 ± 0.2
Y ($\times 10^{6}\,\mathrm{N\,m^{-2}}$)	50 ± 10	35 ± 12	300 ± 35
$\Gamma_{gel/sub}$ ($\times 10^{-3}\,\mathrm{N\,m^{-1}}$)	70 ± 23	62 ± 28	30 ± 25

focusing on the plane of the substrate allows for an accurate observation of the delaminating front which separates a detached region from the adhering one (fig. 2a). In fig. 2a, we clearly observe the evolution of the delaminating front with time and consequently we follow the shrinkage of the adhering region. This is highlighted by the time variations of the dimensionless adhering area and its perimeter in fig. 2b. Comparing the measurements of the adhering region perimeter and a value of the perimeter if this region was circular, we show that the adhering region becomes progressively circular. The process stops when the adhering region does not shrink anymore. Then, the cell adheres to the substrate only by a single region of the surface area denoted by A^f_{adh}. Such regions are well observed in fig. 1b, where each adhering region is encircled by optical interference fringes displaying a layer-substrate air gap. These fringes allow for a precise measurement of the radius of curvature, R, of the buckled region. Measurements of the curvature are shown as a function of the cell surface area in fig. 3. Three different experimental conditions have been considered:

– case 1: desiccation process of the gelled layer at $RH = 46 \pm 1\%$;
– case 2: desiccation process of the gelled layer at $RH = 70 \pm 1\%$;
– case 3: desiccation process of the suspension having an ethanol-water binary mixture solvent at $RH = 46 \pm 1\%$.

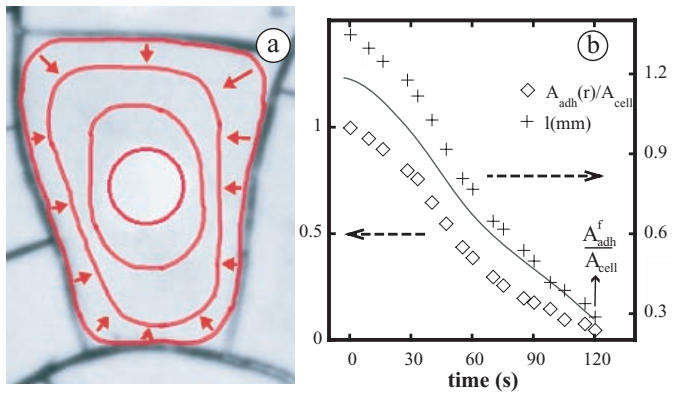

Fig. 2 – Kinetics of the delamination process. a Superposition of images showing the propagation of a delaminating front overprinted by a grey line (the time interval between 2 consecutive lines is 30 s). b Time variations of the adhering to cell area ratio, $A_{adh}(r)/A_{cell}$ and the perimeter, l, of the adhering region. The dark line describes the evolution of the perimeter of the adhering region if it was circular; comparing this line and crosses emphasizes a transition towards a circular adhering region which takes place during the delamination process.

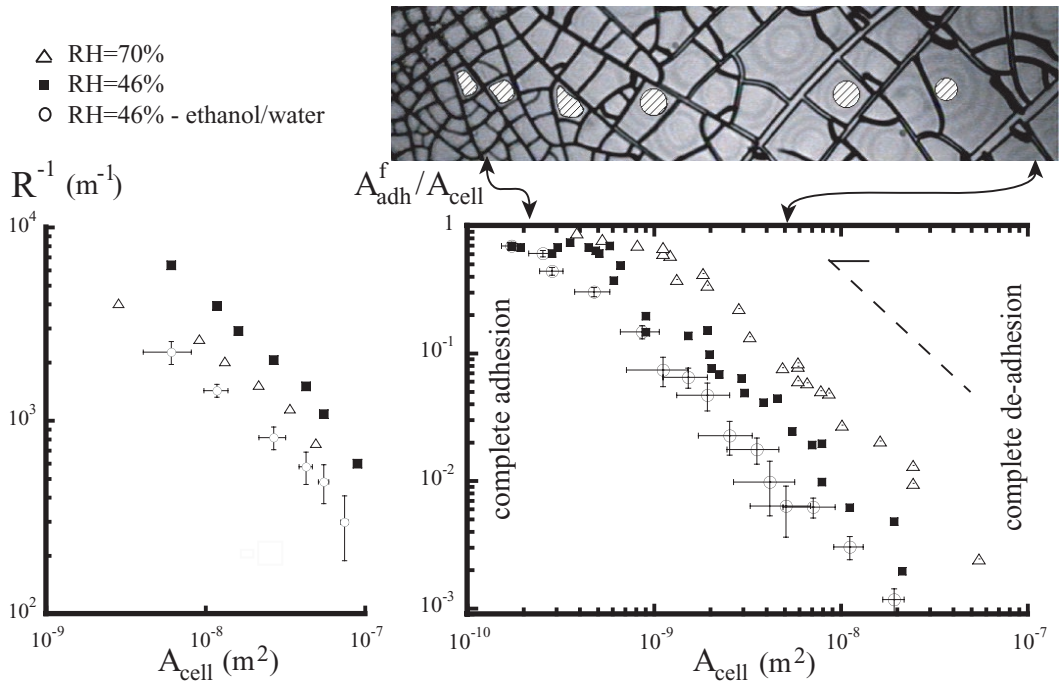

Fig. 3 – Graph in semi-log scale showing the curvature, R^{-1}, of cell surface *vs.* cell area, A_{cell}. Graph in log-log scale showing the ratio A^f_{adh}/A_{cell} as a function of the cell area, A_{cell}, from complete adhesion to complete de-adhesion case. In both graphs, each dot is a statistic and different experimental conditions were studied (rapid drying rate (case 1), low drying rate (case 2) and rapid drying rate of an ethanol-water binary mixture solvent (case 3)). Inaccuracy is only put on measurements performed at $RH = 46\%$ (ethanol-water binary mixture solvent) not to overprint the graph. The scaling law from expression (3) is shown by the dashed line. The digitized image was taken at the final stage of the delamination process: the layer displays a thickness gradient since A_{cell} varies in the range of the axis limited by the arrows. Some adhering regions are overprinted.

As a rule, the larger is the cell size and consequently the thicker is the layer, the lower is the curvature of the buckled region. Indeed, the thicker the layer is, the more rigid it is. Also, fig. 3 shows that the curvature depends on the drying rate of the gel: for a given layer, at low drying rate ($RH = 70\%$) the curvature is lower than that measured at high drying rate ($RH = 46\%$).

The dimensionless adhering area, A^f_{adh}/A_{cell}, was measured as a function of the cell area, A_{cell}, at the final stage of the delamination process; results are shown in fig. 3 for the three cases mentioned. Each dot is a mean value carried out on a layer displaying a constant thickness ranging from $20\,\mu$m to $1000\,\mu$m. Regardless of the experimental conditions (case 1, 2 or 3), for low A_{cell} values, *i.e.* thin layers, the buckling process is rapidly overcome by the adhesion layer/substrate. As a consequence, the delamination process only takes place close to the cell edges, that is the adhering region shrinks only slightly, and the perimeter of the adhering region is not minimized during the competition between buckling and adhesion (an example is shown in the left part of the image on top of fig. 3). For large A_{cell} values, *i.e.* thick layers, the adhering region shrinks more until the formation of a circular adhering region (see the right part of the image on top of fig. 3). Plots in fig. 3 clearly show that the larger is A_{cell}, the

lower is the corresponding adhering area. When the layer thickness is large enough, complete de-adhesion takes place. Moreover, experimental results in fig. 3 show a dependence of the dimensionless final adhering area, A^f_{adh}, on the drying rate of the gelled layer. Indeed, for a given polygonal cell, the final adhering area is larger at low drying rate than that at high drying rate. This simply means that the buckle-driven delamination is less efficient at low drying rate. Also, the role of the solvent was investigated. Thus, the gelation process of nanolatex particles suspension made of ethanol-water binary mixture solvent (desiccation at $RH = 46\%$) was studied (fig. 3). The final dimensionless adhering area is shown to be smaller than that with water solvent. To understand these experimental results, the following model is presented.

The delamination process occurs when the stored elastic strain energy overcomes the adhesion energy of the gel attached to the substrate. This process stops when the elastic strain energy is just overcome by the energy of adhesion. Considering this scenario, let us estimate the energetic contributions which take place. The elastic released energy of the buckled domain is mainly due to the fold limiting the adhering region from the detached one. The theory of elastic plates due to Föppl [13, 14] can be applied under the condition of deformed plates of thickness h, having small h/R ratio. Since the fold is axisymmetric in the final stage of the process (except for certain conditions discussed in the following), the corresponding elastic energy is analogous to that of a fold limiting the contact between a spherical shell and a rigid plane [15]. Thus the elastic energy can be written:

$$U_{fold} = \frac{2C}{3[12(1-\nu^2)]^{3/4}} Y \left(\frac{h}{R}\right)^{5/2} r^3, \tag{1}$$

where C is a constant [16] leading to a prefactor close to 2 when the Poisson ratio, ν, is equal to 0.3 as is the case for most colloidal gels [10], Y is the Young modulus of the delaminating cell and r denotes the radius of the adhering region that is supposed to be axisymmetric in expression (1). From expression (1) we notice that it is energetically favourable to minimize the length of the fold in order to diminish the elastic energy of the system as is shown in the experimental measurements in fig. 2b. However, this energy competes with the work of adhesion, U_{adh}, which exhibits resistance to the detachment of the layer because the interfacial crack leads to the formation of new surfaces of area, $A_{cell} - A_{adh}(r)$, according to Griffith theory [17]:

$$U_{adh} = 2\Gamma_{gel/sub}(A_{cell} - A_{adh}(r)), \tag{2}$$

where $\Gamma_{gel/sub}$ is the interfacial energy per unit area, *i.e.* the one needed to propagate a crack between the gelled layer and the substrate. In the case of a quasistatic process it allows for the determination of $\Gamma_{gel/sub}$ from the measurements of the geometrical quantities A_{adh} and R, both being function of the cell area and consequently of the layer thickness. At the final stage of the delamination process, $A^f_{adh} = A_{adh}(r_f) = \pi r_f^2$. Equilibrium of forces defined as $F_{adh} = \mathrm{d}U_{adh}/\mathrm{d}u$ and $F_{buckl} = \mathrm{d}U_{buckl}/\mathrm{d}u$ (see fig. 1c) yields

$$A^f_{adh}(A_{cell}) = \frac{96\pi^2 3^{1/2}(1-\nu^2)^{3/2}}{C^2} \left(\frac{\Gamma_{gel/sub}}{Y}\right)^2 \left(\frac{R(A_{cell})}{h(A_{cell})}\right)^5, \tag{3}$$

taking into account $A_{cell} = \alpha h^2$. Expression (3) gives a scaling law to fit the experimental results in fig. 3, A^f_{adh}/A_{cell} as a function of A_{cell}, under certain conditions: cell size not too small ($A_{cell} > (20\,\mu\mathrm{m})^2$) otherwise the adhering region is usually not circular at the final stage of the delamination process (expression (3) is not valid for $A^f_{adh}/A_{cell} \simeq 1$); cell size not too large ($A_{cell} < (200\,\mu\mathrm{m})^2$) since low $\frac{h}{R}$ is required [13, 14] (typically $\frac{h}{R} < 10^{-1}$). As shown in fig. 3, the final dimensionless adhering area is strongly dependent on the experimental

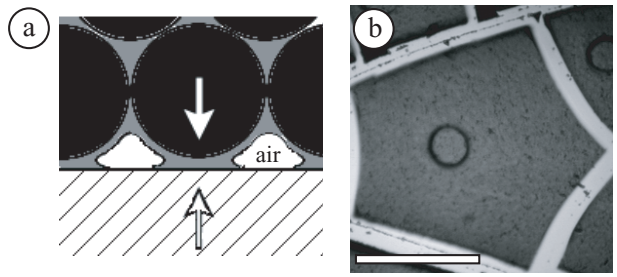

Fig. 4 – a Sketch of a package assembly of particles (in black) with pores filled of solvent (grey) close to the gel/substrate interface. Vertical arrows illustrate normal capillary force due to air-in-liquid capillary bridge. b The digitized image shows a circular crack formed inside the adhering region 15 minutes after the end of the delamination process (bar = 100 μm).

conditions (case 1, 2 or 3). In this way by changing the drying rate of the gel, or the quality of the suspension solvent, the mechanical properties of the drying gel are modified. As a consequence, the Young modulus, thickness variations of the crack spacing ($A_{cell} \approx \alpha h^2$) and also the curvature (R^{-1}) of gelled cells have to be measured in each case. Measurements are presented in table I for each experimental condition. Also, we observe that at low drying rate the crack spacing is larger than at high drying rate [18]. In addition, the presence of ethanol in the solvent makes the gel more rigid (Y higher) in agreement with theoretical predictions in ref. [10]. Fitting our experimental results with expression (3) allows us to determine $\Gamma_{gel/sub}$.

For gels dried at $RH = 46\%$ (according to case 1), fitting measurements with expression (3) leads to an energy of adhesion: $\Gamma_{gel/sub} = 70 \pm 23\,\mathrm{mN\,m^{-1}}$ (additional observations show that no significant change is observed by changing the substrate surface —glass slide cleaned in different ways or wafer substrate). For gels dried at lower drying rate, $RH = 70\%$, (according to case 2), no significant change is obtained in the energy of adhesion since $\Gamma_{gel/sub} = 62 \pm 28\,\mathrm{mN\,m^{-1}}$. At last, for gels made of ethanol-water binary mixture solvent (according to case 3), best fit leads to $\Gamma_{gel/sub} = 30 \pm 25\,\mathrm{mN\,m^{-1}}$. Interestingly, this last value can be compared with the surface tension of the colloidal suspension before desiccation. Measurements using the Wilhelmy plate method give $42 \pm 8\,\mathrm{mN\,m^{-1}}$ for the surface tension of the suspension with ethanol-water solvent (case 3), instead of $65 \pm 5\,\mathrm{mN\,m^{-1}}$ for the suspension without ethanol (cases 1 and 2). These results suggest the adhesion between the gel and the substrate be related to a capillary process close to the gel/substrate interface. Indeed, the presence of air in the drying gel is assumed to compensate solvent loss during the drying process. In this way, an air-in-liquid capillary bridge can exist in the porous structure, in the vicinity of the substrate, as illustrated in fig. 4a. Such capillary bridges can be responsible for strong attractive interaction [19]. This can be emphasized by a simple observation: when the solvent is completely removed from the gel, after a duration close to 24 hours, the layer does not adhere anymore to the substrate, even if the curling deformation of the cells is still the same than just after the delamination process.

Finally, let us focus on the residual stress remaining inside the adhering regions of the layer. On the one hand, observation of polygonal cracks between cross-polarized light reveals birefringence of the adhering regions. The birefringence effect is induced by residual stresses due to strong adhesion between gel and substrate. On the other hand, a new generation of cracks can form inside the adhering region, whereas no crack can nucleate in the detached part of the gel: fig. 4b shows a circular crack inside the adhering region of a polygonal cell as the evidence of important stress inside the adhering region. It has to be noticed that spiral-cracks

formation inside a polygonal cell has been recently studied [8]. In this last case, spiral cracks form during the delamination process of the polygonal cell. In the present study, this new generation of crack patterns forms well after the end of the delamination process.

As a conclusion, the present study deals with the stage which follows the formation of cracks delimiting polygonal cells in a gelled layer. The partial delamination process of cells is induced by desiccation of the gel and is studied in different experimental conditions. Particularly, the variation of adhering area to the cell area has been studied as a function of the cell thickness. For thin layers, the delamination process is difficult and a detached region is localized close to the crack edges. However, for thicker layers, the adhering region is preferentially circular at the final stage of the delamination process. Our model system exhibits well-controlled physicochemical properties. Indeed, mechanical properties can be modified and deformations can be accurately measured in order to test the relevance of a theory based on the competition between buckling process and interfacial crack propagation.

* * *

I would like to thank M. Adda-Bedia, C. Allain, K. Sekimoto, H. Auradou and A. Chevalier for useful discussions.

REFERENCES

[1] Bard J. B., in *Morphogenesis* (Cambridge, University Press) 1992.
[2] Bird P., *J. Geophys. Res.*, **84** (1979) 7561.
[3] Lewis P. H. *et al.*, *IEEE Trans. Image Processing*, **13** (2004) 302.
[4] Hutchinson J. W. and Suo Z., *Adv. Appl. Mech.*, **29** (1992) 62.
[5] Gioia G. and Ortiz M., *Adv. Appl. Mech.*, **33** (1997) 119.
[6] Audoly B., *Phys. Rev. Lett.*, **83** (1999) 4124.
[7] Atkinson A. and Guppy R. M., *J. Mater. Sci.*, **26** (1991) 3869; Groisman A. and Kaplan E., *Europhys. Lett.*, **25** (1994) 415; Allain C. and Limat L., *Phys. Rev. Lett.*, **74** (1995) 2981; Komatsu T. S. and Sasa S., *Jpn. J. Appl. Phys.*, **36** (1997) 391; Colina H. and Roux S., *Eur. Phys. J. E*, **1** (2000) 189.
[8] Neda Z., Leung K.-t., Jozsa L. and Ravasz M., *Phys. Rev. Lett.*, **88** (2002) 5502.
[9] Deegan R. D. *et al.*, *Nature*, **389** (1997) 827.
[10] Brinker C. J. and Scherer G. W., in *Sol-Gel Science* (Academic Press, New York) 1990, pp. 453-488.
[11] Malzbender J., den Toonder J. M. J., Balkenende A. R. and de With G., *Mater. Sci. Engin.*, **R36** (2002) 42.
[12] Zarzycki J., *J. Non-Cryst. Solids*, **100** (1988) 359.
[13] Föppl A., *Vorlesungen tech. Mech.*, **5** (1907) 132.
[14] Landau L. and Lifshitz E. M., in *Theory of Elasticity*, 3rd edition (Pergamon Press, New York) 1986.
[15] Pauchard L. and Rica S., *Philos. Mag. B*, **78** (1998) 225.
[16] Audoly B. and Pomeau Y., in *Elasticity and Geometry: From Hair Curls to Nonlinear Response of Shells* (Oxford University Press) in press.
[17] Griffith A. A., *Trans. R. Soc. London*, **221** (1920) 163.
[18] Parisse F., Thesis, Université Paris XI (1997).
[19] Mastrangelo C. H., *Tribol. Lett.*, **3** (1997) 223.